OPEN ACCESS
IOP Publishing
Classical and Quantum Gravity
Class. Quantum Grav. **42** (2025) 055013 (22pp)
https://doi.org/10.1088/1361-6382/adaf00

Advanced charge control dynamics simulation for the LISA gravitational reference sensor

Samantha Parry Kenyon[1,*], Stephen Apple[2], John Siu[2], Peter J Wass[2] and John W Conklin[2]

[1] Aerospace and Ocean Engineering, Virginia Tech, Blacksburg, VA, United States of America
[2] Mechanical and Aerospace Engineering, University of Florida, Gainesville, FL, United States of America

E-mail: spkenyon@vt.edu

Received 15 November 2024; revised 4 January 2025
Accepted for publication 27 January 2025
Published 17 February 2025

Abstract

A gravitational wave detector in space, the Laser Interferometer Space Antenna (LISA) will be able to detect gravitational waves in the frequency range of 0.1 mHz–1 Hz, adding to humanity's knowledge of the dark cosmos. The LISA gravitational reference sensor contains a test mass (TM) and is used to determine the local inertial reference frame and as endpoints for the interferometry. The TM is surrounded by an electrode housing to detect changes in TM position and orientation, which is fed back to the spacecraft thrusters for drag-free control. As seen on LISA Pathfinder, the TM builds up charge over time from the space environment and needs to be discharged in order to keep the resulting force noise as low as possible. The operation of intelligently discharging the TM is known as charge control, and is one area of improvement to be explored for LISA. To explore new methods of TM discharge, UV LEDs will be pulsed synchronized with an existing 100 kHz high frequency electric field to facilitate photoelectron current direction and to achieve lower UV light powers by duty cycling. This paper addresses new pulsed methods for the LISA Charge Management System, which require in-depth modeling, analysis, and testing because space environment validation will not be possible prior to LISA

* Author to whom any correspondence should be addressed.

Original Content from this work may be used under the terms of the Creative Commons Attribution 4.0 licence. Any further distribution of this work must maintain attribution to the author(s) and the title of the work, journal citation and DOI.

© 2025 The Author(s). Published by IOP Publishing Ltd

launch. Therefore, it is necessary to model the dynamics of charge movement to determine the force noise contribution of pulsed continuous charge control. The charge dynamics model is described, and simulation results featured for charge control efficacy in a deep space radiation environment. Experimental testing of the simulation results could be done in the University of Florida Torsion Pendulum, a key technology to testing GRS performance in a space-like environment.

Keywords: gravitational wave detection, gravitational reference sensor, inertial sensing, charge control, contact free discharge, physics-based model

1. Introduction: the LISA mission and the charge management system

Space inertial sensors include both gyroscopes and accelerometers that can measure both a spacecraft's attitude and relative position. The relative position over time is calculated through direct measurement of the acceleration of the sensor. They are typically composed of a proof mass, or test mass (TM) in free-fall, surrounded by capacitive electrode housing to detect relative position over time and to apply small forces to the TM during spacecraft maneuvering. Related sensors and technology was imperative for missions in the past, such as the accelerometers flown on CHAMP (2000) [1], GRACE (2002) [2], GOCE (2009) [3] and GRACE-FO (2010) [4] for earth geodesy measurements, the gyroscopes flown on Gravity Probe B (2004–2005) [5] for tests of General Relativity, and the differential accelerometers flown on MICROSCOPE (2016–2019) [6] to test the equivalence principle. Looking ahead, advanced inertial sensor technology is needed for the Laser Interferometer Space Antenna (LISA) [7] to detect gravitational waves in space, and has been proven to be a key technology for the mission due to the inclusion of inertial sensor noise performance demonstrations in the LISA Pathfinder (LPF) mission (2015–2017) [8, 9]. A number of improvements are being made to the charge management system of precision space inertial sensors for the success of LISA and upcoming next-generation earth geodesy missions.

For LISA, measuring the relative position displacement over time of a pure geodesic orbit is crucial to successful measurement of a gravitational wave (GW). GWs are 'ripples' in space-time due to high energy events in the Universe and can travel at the speed of light undisturbed [10]. They stretch and compress space-time at a frequency determined by their source. The LISA mission is a ESA/NASA joint space mission that will be the first space-based GW observatory, with an envisioned launch in the mid-2030 s. It will significantly contribute to knowledge of the dark cosmos through detection of new GW events together with ground-based observatories LIGO and Virgo [11]. To detect GW in the lower frequency range of 0.1 mHz to 1 Hz, LISA will be composed of three drag-free spacecraft flying in roughly an equilateral triangle formation exchanging information via six one-way laser links for redundancy, polarization and location resolution. The observatory will be a Michelson-like interferometer with arm lengths 2.5×10^6 km. LISA's barycenter will approximately follow the Earth in its orbit around the Sun, while spinning on its axis. It will have a strain sensitivity down to $10^{-20}\ \frac{1}{\sqrt{\text{Hz}}}$ at 1 mHz, corresponding to a relative length resolution of $10^{-10}\ \frac{\text{m}}{\sqrt{\text{Hz}}}$ [7]. To ensure drag-free motion, each spacecraft contains two inertial sensors, which the spacecraft moves and orients itself around, like a position anchor. It is shielded from solar radiation pressure to ensure a strain measurement is dominated by a GW [10]. The inertial sensors are also used as the end points of the interferometer whose displacement difference is precisely measured to detect GWs.

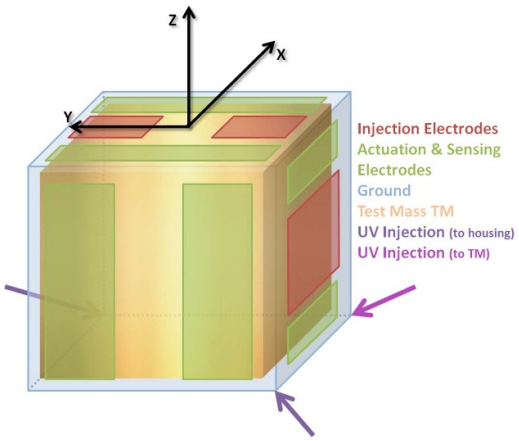

Figure 1. Drawing of the LPF GRS electrode orientation of total quantity 18. Note that the orientation is the same on each electrode housing opposing surface.

1.1. Gravitational reference sensor (GRS)

The inertial sensor used on LPF, the technology development mission for LISA to test its projected performance, is called the GRS [8]. Due to LPF success, LISA is projected to use the same sensor. The GRS is composed of a cubic TM surrounded by an electrode housing (EH) necessary for position and orientation sensing, TM actuation, and electric field injection through a capacitor sensing scheme as illustrated in figure 1. Correlating the capacitance readout with the position of the TM, the spacecraft is able to precisely move and orient itself to keep the TM centered using 6 degree of freedom micro-newton thrusters [10]. The drag-free system constrains spacecraft movement largely to geodesic motion, as long as all other external forces on the TM are mitigated. The surface of the TM also acts as the end mirror for the interferometer, thus the EH can actuate the TM to maintain its attitude to ensure that the beam is normal to the reflection surface. For this reason, each spacecraft will have two GRS's on-board in order to create six unique laser links for the constellation. The injection electrodes can induce necessary electric fields to perform position localization at high frequencies where noise is low.

The GRS is surrounded by a vacuum chamber that will be vented to the space environment. The TM is a 46 mm cube, of mass 1.96 kg made up of a gold–platinum alloy, selected for its low magnetic qualities and high density. All internal surfaces are coated in gold, which is chosen due to its homogeneous electrostatic surface properties, as well as its reflectivity at infrared wavelengths. Necessary to successful GRS performance to measure displacement changes between TMs for a GW measurement, all sources of noise within the frequency band of the measurement must be reduced. They must remain below the required acceleration noise requirements between opposing TMs, which is lowest at $3 \times 10^{-15}\ \frac{\mathrm{ms}^{-2}}{\sqrt{\mathrm{Hz}}}$ at 1 mHz [10].

Because the signal is dependent on frequency, constant/DC forces do not affect the strain measurement. However, any varying force over time, when converted to the frequency domain, will have a contribution in the LISA band of 0.1 mHz–1 Hz. The TM experiences many forces, some of which are electrostatic. Because the TM and associated EH have different electric potentials, which change over time, the TM experiences both Lorentz and Coulomb forces. The magnetic Lorentz forces remain below requirement due to TM material selection limiting the magnetic susceptibility and remnant moment of the TM, as well as shielding the GRS

in a conducting enclosure [12]. However, to mitigate the Coulomb electric field forces, more complex systems are required.

1.2. History of charge control and UV LEDs

Controlling the charge of the TM is critical to the sensitivity of LISA, as any induced frequency-dependent force on the TM that is not caused by acceleration due to a passing GW could cause an in-band noise contribution, as detailed in section 2. A TM Charge Management System (CMS) may employ a small, $\sim 10\mu$m diameter grounding wire to discharge the TM. However, the method of using a gold contact wire in missions such as GRACE, GRACE-FO, and GOCE produce noise that exceeds the acceleration noise requirement of LISA [1, 4]. Therefore, the photoelectric effect is exploited as a non-contact method of discharging. The work function for pure Au is 5.2 eV, which is the corresponding energy that the incident light must have to emit electrons, thus requiring a particular wavelength of $\leqslant$239 nm [13]. When Au-coated surfaces are exposed to air and subject to water and hydrocarbon contaminants, the work function lowers to approximately $\geqslant 4.3 \pm 0.4$ eV [14, 15], which requires a wavelength of $\leqslant \sim$289 nm. Therefore, deep UV light is the suitable candidate for discharging the TM [16]. LPF primarily used Hg lamps of dynamic range 300:1 in a DC intermittent mode, when the light would shine continuously every 2–3 weeks to discharge the TM, causing science mode to pause [17].

The LISA CMS will utilize UltraViolet light emitting diodes (UV LED) because of their larger dynamic range of 10^7 (from about 10^{-6} to 10^{-13} W [18]) achieved by varying the power amplitude and pulsing them at high frequencies. The ability to achieve lower light levels limits shot noise and therefore TM acceleration noise [19]. Pulsing the UV light exploits a pre-existing GRS 100 kHz sinusoidal electric field, which is used to shift the TM position and orientation from DC to high frequency. To facilitate electron movement in the desired direction, the UV pulses are generated in-phase or out-of-phase with this field. Synchronizing with the 100 kHz field eliminates the need to apply DC voltages to facilitate the direction of charge current. This also means that the direction of photoelectron current flow can still be chosen when shining UV light on either the TM or surrounding housing, eliminating the influence of reflectivity and quantum yield of the Au-coated surfaces and provides more control over intended electron movement. The described method is known as AC [19], synchronized [20], or pulsed charge control. UV LEDs are also a viable candidate due to promising lifetime performance results in recent laboratory tests [18].

1.3. Motivation for developing charge dynamics model

In order to understand how charge within the GRS move, knowledge of many parameters must be known and understood. Previous work has been done to simulate space radiation as compared to LPF data [21, 22] and using simulated space radiation to model charge movement in a similar GRS [23]. Additionally, control systems have been designed, specifically a model reference adaptive control system and a PID controller respectively for a similar GRS [24, 25]. To address the uncertainty of the system, other works start with a simplified physics-based model and extrapolate uncertainties using advanced methods [26]. However, these works do not simulate the performance of the CMS in the frequency domain to motivate the need for pulsed charge control as compared to intermittent DC charge control.

A simplified analytical model has been developed for the photoelectron currents within the LISA GRS to assist in explaining discharge phenomenon, both predicted and measured [27, 28]. This model captures the dependence on the UV light spectrum, surface properties

of the gold-coated surfaces (quantum efficiency, work function), angle of UV light and how it is reflected among the three types of surfaces within the GRS (housing, TM, electrodes), GRS geometry, and other features characteristic of the LISA GRS. The work in this paper uses the efforts published in [27] to develop a dynamical TM charge simulation using measured apparent yield (AY) curves (described in section 2.1) that can inform calibration of the charge control and inform assessment of performance with respect to requirements. It also uses measured environmental charging rates from LPF, rather than simulated. Additionally, no active control system is necessary for maintaining low TM potentials.

2. CMS methods

To understand the motivation for a CMS, an analysis will be done of the effect of Coulomb forces in the LISA GRS. Thus, we start with Coulomb's Law:

$$\overrightarrow{F} = q\overrightarrow{E}. \tag{1}$$

Here, q is the charge on the TM, $\overrightarrow{E}$ is the net electric field within the GRS that the TM is subject to, and $\overrightarrow{F}$ is the force that the TM undergoes. We are interested in the force contribution the TM experiences in the sensitive measurement direction, $\hat{x}$, because this is the direction of the interferometry distance measurement [29]. It has been shown in [30] that this force F_x along the sensitive measurement axis x can be modeled as a coupling between the TM charge q and an electric potential on the TM or EH. We parameterize this potential as an equivalent electric potential on a single EH x-electrode Δ_x. When talking about the electric field potential Δ_x, it is assumed that the potential is determined relative to the grounded GRS housing. In a symmetric sensor with a centered TM and in the absence of other applied voltages, in the sensitive measurement direction equation (1) becomes [30]:

$$F_x = qE_x \approx -\frac{q}{C_T}\left|\frac{\partial C_x}{\partial x}\right|\Delta_x. \tag{2}$$

Here, C_{T} and C_x are the total capacitance of the TM to ground and the capacitance between the TM and the x-electrode, respectively. Force noise over a particular frequency band arises from either a fluctuating TM charge coupling with the mean value of Δ_x or a fluctuating Δ_x coupling with the mean TM charge. To illustrate this concept, both q and Δ_x produce noise, meaning they vary over time, and we can write,

$$q = q_o + \delta q\,(t) \tag{3}$$

$$\Delta_x = \Delta_{o,x} + \delta\Delta_x\,(t)\,. \tag{4}$$

Here, q_o is the DC contribution of the TM charge, $\delta q(t)$ is the time-dependent charge noise, $\Delta_{o,x}$ is the DC contribution of the electric field potential in the $\hat{x}$ direction, and $\delta\Delta_x(t)$ is the time-dependent noise contribution of the electric potential in the $\hat{x}$ direction. Incorporating equations (3) and (4) in equation (2),

$$F_x = \frac{|\delta C_{\mathrm{T}}/\delta x|}{C_{\mathrm{T}}}\left[q_o\Delta_{o,x} + \Delta_{o,x}\delta q\,(t) + q_o\delta\Delta_x\,(t) + \delta q\,(t)\,\delta\Delta_x\,(t)\right]. \tag{5}$$

The first term, $q_o\Delta_{o,x}$, is a DC contribution and does not pollute the frequency band of the measurement. If $\delta q(t)$ and $\delta\Delta_x(t)$ are small, the last term $\delta q(t)\delta\Delta_x(t)$ is two small contributions multiplied together, which is also negligible. The main sources of noise contribution in the LISA measurement frequency band are the second and third terms.

The second term $\Delta_{o,x}\delta q(t)$ begins to pollute the measurement if the net DC electric field $\Delta_{o,x}$ is large and it couples with the charge noise $\delta q(t)$ which has a frequency contribution. The term becomes acceptable if the net DC electric field is reduced to below the required level, which can be done by measuring the inherent electric field within the GRS and applying a counter-field via the electrodes to compensate for it. Motivated to accurately and quickly measure Δ_x, experiments have been performed with advanced methods beyond LPF [31].

The third term, $q_o\delta\Delta_x(t)$, like the second term, pollutes the science measurement if the charge of the TM q_o is large and it couples with the small electric field noise term $\delta\Delta_x(t)$, which is still present even after electric field compensation. The term can be reduced if the TM charge stays low. However, keeping the TM charge low is a challenge because the space environment naturally charges the TM over time due to radiation (cosmic rays and solar radiation) that pass through the spacecraft and accumulate on the TM [10]. Therefore, it is necessary to discharge the TM from the inevitable charge accumulation from the space environment.

2.1. AY curve

An AY curve describes the rate of TM charge per UV light power ($\dot{q}/P_{\mathrm{UV}}$) as a function of the TM potential (V_{TM}). The curve captures contributions due to geometry, surface properties, and sensor capacitance within the GRS that are theoretically captured in the charge control model work [27]. AY curves also describe where the TM equilibrium point is. When the AY is zero, which means there is no net photoelectron current due to UV light, the corresponding TM potential is at equilibrium. It is the AY curve x-axis crossing. AY curves have been measured for both LPF data [13] and for both torsion pendulums that the GRS team uses at the University of Trento, Italy, and the University of Florida [32, 33] which can be seen in figure 2. The TM port UV light reflects off the TM with a 75° angle of incidence relative to the surface normal and is centered on one of the sensing electrodes(specifically Y2+), and the AC port UV light reflects off the TM and onto the $\mathrm{Y3_{inj}}$ electrode with a 30° angle of incidence. These curves were obtained with using DC continuous light, not pulsed light, and voltages were applied to resolve the ends of the S-shape curve when necessary. The data was fit to an empirical model that represents the behavior well.

The S-curves were fit to an analytical sigmoid function to empirically model their behavior. The analytical expression is as follows:

$$\mathrm{AY} = \mathrm{AY_{min}} + (\mathrm{AY_{max}} - \mathrm{AY_{min}})\left(1 + \mathrm{e}^{k(V-x_o)}\right)^{-a}. \tag{6}$$

Here, $\mathrm{AY_{min}}$ and $\mathrm{AY_{max}}$ are the limits of the curve, x_o shifts the curve from left to right, and k and a determine the slope and the level of symmetry of the S-curve. The function was fit to the data via a MATLAB built-in function 'fminsearch' to find the constants k, x_o, and a, while $\mathrm{AY_{min}}$ and $\mathrm{AY_{max}}$ were solved using a linear least squares fit. The best fit models are plotted against the measured AY for the TM and AC port in figure 2. The resulting standard deviation of the residuals for the curve fits are 1.02×10^{-8} for the TM port curve, 1.09×10^{-8} for the AC port curve. Fitting the pendulum AY curves to a function is helpful for understanding how the UV light phase alters the equilibrium potential of the TM.

The TM potential is in equilibrium when the AY is zero. Near equilibrium, the AY can be described as a linear function of V_{TM} with slope β as described in section 3. Thus, the TM potential tends exponentially to equilibrium with a decay constant α also described in section 3. If the UV power is in units of W, then the decay constant can be written as:

$$\alpha = \frac{\beta\lambda P_{\mathrm{UV}}}{C_{\mathrm{T}}hc}. \tag{7}$$

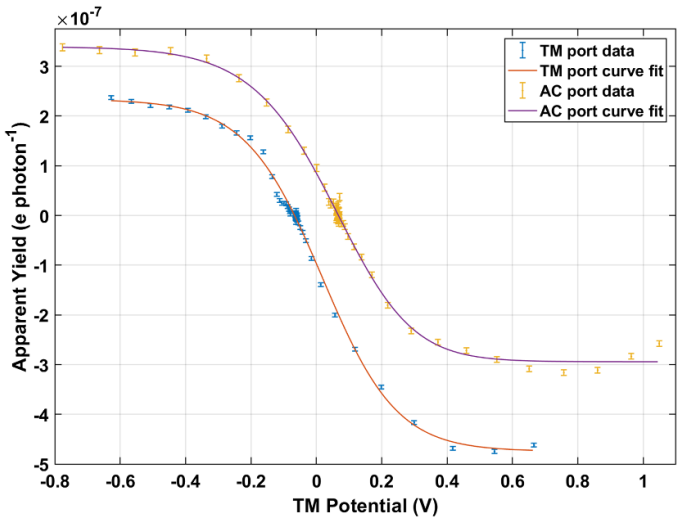

Figure 2. Measured UV light AY curves using the TM and AC injection ports with their fitted empirical models.

Here, $\lambda = 250$ nm is the wavelength of the UV light, h is the Planck constant, and c is the speed of light. Therefore, the AY curves allow the analytical charge model to be solved for as close to explicit as possible. The expression is then numerically solved to generate an approximate solution, and is detailed in the following sections.

3. Analytical charge model

To describe the TM charge as an analytical expression, the AY curve for a particular UV light injection port can be approximated as linear at TM potentials between approximately -0.1 V to 0.1 V in the form:

$$\frac{\dot{q}_{\mathrm{cc}}}{P} = \beta\,(V_{\mathrm{TM}} - V_{\mathrm{eq}})\,. \tag{8}$$

Here, β is the constant slope of the near-linear function, $\dot{q}_{\mathrm{cc}}$ is the electron discharge rate due to charge control in electrons per second, P is the UV power in photons per second, and V_{eq} is the equilibrium point voltage, i.e. the y-axis crossing. If the inertial sensor was just a free-floating TM surrounded by a uniform housing, the relationship between charge q and V_{TM} is governed by the general capacitor equation:

$$V_{\mathrm{TM}} = \frac{q}{C_{\mathrm{T}}}, \tag{9}$$

where the charge q is in units of Coulombs and C_{T} is the total TM capacitance relative to ground. Due to the LISA GRS being composed of many electrodes that each have their own respective capacitance with the TM, the capacitance equation applied in the LISA-like GRS is the following [29]:

$$V_{\mathrm{TM,uncentered}} = \frac{q}{C_{\mathrm{T}}} + \frac{\sum V_i C_i}{C_{\mathrm{T}}}. \tag{10}$$

Here, C_i is the capacitance between the TM and the ith electrode. Under the assumption that the TM is centered within the GRS, and the applied voltages are equal and opposite for a pair of electrodes with the same capacitance, then equation (10) becomes equation (9) in the LISA band. This equation is crucial because the TM charge is often called the TM potential as well. These interchangeable names are synonymous governed by the constant C_{T}.

When the light is pulsed in phase or out of phase, the TM potential voltage changes due to the phase of the UV light along the sinusoidal 100 kHz injection signal. This effectively applies an additional voltage on the TM within the GRS. The additional voltage can be approximated as an additional charge called q_{ac} governed by equation (9): $V_{\mathrm{TM,ac}} = q_{\mathrm{ac}}/C_{\mathrm{T}}$. Note that variable that q_{cc} is the TM charge due to charge control with no applied voltages, also governed by equation (9): $V_{\mathrm{TM,cc}} = q_{\mathrm{cc}}/C_{\mathrm{T}}$. Thus voltage V_{TM} can be approximated as a sum of the following two voltages and equation (9) becomes

$$V_{\mathrm{TM,total}} = V_{\mathrm{TM,cc}} + V_{\mathrm{TM,ac}} = \frac{1}{C_{\mathrm{T}}}\, q_{\mathrm{cc}} + \frac{1}{C_{\mathrm{T}}}\, q_{\mathrm{ac}}. \tag{11}$$

Substituting equation (11) and the relationship between TM equilibrium voltage to equilibrium charge $V_{\mathrm{eq}} = q_{\mathrm{eq}}/C_{\mathrm{T}}$ into equation (8),

$$\dot{\mathrm{q}}_{\mathrm{cc}} = \frac{\beta}{C_{\mathrm{T}}} P\left(q_{\mathrm{cc}} + q_{\mathrm{ac}} - q_{\mathrm{eq}}\right). \tag{12}$$

This describes the rate of TM charge with respect to charge rather than voltage, with q_{cc} as the independent variable. Expressing equation (12) as a simple first order ordinary differential equation,

$$\dot{q}_{\mathrm{cc}} = \alpha\left(q_{\mathrm{cc}} + q_{\mathrm{ac}} - q_{\mathrm{eq}}\right) \tag{13}$$

where $\alpha = \beta\, P/C_{\mathrm{T}}$ when UV power is in units of photons/s (P), and α is equal to equation (7) when UV power is in units of Watts (P_{UV}). The solution to this differential equation assuming α, q_{ac}, and q_{eq} are constant with initial condition $q_{\mathrm{cc}}(0) = q_o$ is the following.

$$q_{\mathrm{cc}} = \left(q_o - q_{\mathrm{eq}} + q_{\mathrm{ac}}\right) e^{\alpha t} + q_{\mathrm{eq}} - q_{\mathrm{ac}}. \tag{14}$$

This is an expression for the charge of the TM in terms of capacitance, UV power, slope β from figure 2, and time.

The solution of this ordinary differential equation is an exponential function, which indicates the charge of the TM over time will decay exponentially to $q_{\mathrm{eq}} - q_{\mathrm{ac}}$. If the desired TM charge is 0 V, it will decay towards zero when $q_{\mathrm{eq}} = q_{\mathrm{ac}}$. Although the equilibrium charge is a fixed parameter dependent on the GRS properties, the charge contribution due to pulsing UV light q_{ac} is adjustable based on pulsed UV light phase, power, and duration. Thus, precise control of the equilibrium point of the TM is possible through pulsed charge control.

If one must consider the total contribution of the TM charge due to the space radiation environment, then equation (13) becomes the following:

$$\dot{q} = \dot{q}_{\mathrm{cc}} + \dot{q}_{\mathrm{env}} = \alpha\left(q_{\mathrm{cc}} + q_{\mathrm{ac}} - q_{\mathrm{eq}}\right) + \dot{q}_{\mathrm{env}}. \tag{15}$$

If $\dot{q}_{\mathrm{env}}$ is considered a constant, R [e/s], then the solution to equation (15) with the initial condition $q(0) = q_o$ is:

$$q = \left(q_o - q_{\mathrm{eq}} + q_{\mathrm{ac}} + \frac{R}{\alpha}\right) \mathrm{e}^{\alpha t} + q_{\mathrm{eq}} - q_{\mathrm{ac}} - \frac{R}{\alpha}, \tag{16}$$

which can also simplify to the following:

$$q = \left(q_o - q'_{\rm eq}\right) {\rm e}^{\alpha t} + q'_{\rm eq}, \tag{17}$$

where $q'_{\rm eq} = q_{\rm eq} - q_{\rm ac} - \frac{R}{\alpha}$. Since the environmental charge rate is an independent variable, to control the net charge q and to make it exponentially decay to a desired equilibrium voltage, the net UV power P and pulsed UV light phase and duration to determine $q_{\rm ac}$ can be controlled to generate a desired $q'_{\rm eq}$. This result implies that, if your pulse properties are such that $q_{\rm ac} = q_{\rm eq} - \frac{R}{\alpha}$, then your equilibrium voltage is zero.

4. Numerical charge model

Understanding how TM charge changes over time with respect to GRS properties, UV light parameters, and the radiation environment is critical to knowing how an advanced pulsed charge control system will work in space. Since LPF was only able to test DC charge control in space [13], having a dynamics model to understand this advanced system is important to the LISA mission. Thus, a model in MATLAB was developed to simulate the pulsed charge control system.

The analytical equation (17) cannot be solved explicitly because in reality, the radiation environment charging is not a constant. Its dependence on time is a challenge to model, and although data from LPF on the environment charging rate of the TM is used in the simulation, it cannot be known *a priori* for LISA. Not only does this not allow the use of the analytical solution for the TM charge, but also the shot noise contribution, an important factor in the TM charge noise, is not known explicitly. To get an accurate representation of the charge control effect in the frequency domain due to environment noise and shot noise, a numerical expression is used in the simulation. The linear approximation of the AY curves thus is no longer needed, since the linear approximation was only a part of the assumptions for the analytical solution. Therefore, the full AY S-curve data was used in the numerical model to capture any nonlinear effects. The numerical expression to capture the change in charge at every time step is the following:

$$\delta q = \sum \left[{\rm AY}\left(q\left(t-1\right)\right) \cdot P_{\rm pulse}\right] + \left[R + \delta R\right] + SN \tag{18}$$

where $P_{\rm pulse}$ is a function of ϕ, $\delta\phi$, DC, $P_{\rm UV}$, and $\delta P_{\rm UV}$). The variable $P_{\rm pulse}$ is a vector so it can capture the effects of pulse timing and noise effects. It is composed of the UV light power $P_{\rm UV}$ averaged over one period of the 100 kHz sinusoid (10 μs) with a 1 ns step size as well. The $P_{\rm pulse}$ vector contains zeros when the light is off, and a fraction of the total power when the light is on. Thus, it is dependent on phase ϕ and phase noise $\delta\phi$, duty cycle DC, and power amplitude noise $\delta P_{\rm UV}$. If the vector $P_{\rm pulse}$ was summed, it would equal the average UV power. The variable AY is also a vector of AYs as governed by the AY curve that is provided to characterize the GRS of interest. It is dependent on the voltage of the previous TM charge plus the voltage at 1 ns intervals along the 100 kHz sinusoid. The AY and the $P_{\rm pulse}$ vectors are multiplied together and summed to produce a scalar of the effective AY through the pulse duration. Due to applying vector math to obtain the effective AY, the noise parameters are approximated every second because they are assumed to be constant over the course of each second interval. This means that the resolution of the noise due to pulsed discharge is limited to one second. Additionally in equation (18), the average environment rate R, environment noise δR, and shot noise SN are included. The shot noise is approximated determining the AY limits for the particular UV injection port's S-shape curve and obtaining the minimum of the

absolute value. The minimum of the AY is then multiplied by a factor of P_{UV} to determine the standard deviation of the shot noise.

5. Force noise

As mentioned previously, the GRS TM experiences both Lorentz and Coulomb forces. The Lorentz forces are reduced due to TM material selection. However, the Coulomb forces require a CMS to be properly managed. Recall from equation (5) that the net force the TM experiences in the sensitive $\hat{x}$ direction is a combination of charge, electric field, and the noise that they both experience:

As discussed previously, the shot noise $\delta q(t)$ and the net fluctuating electric potential fields $\delta\Delta_x(t)$ when coupled to their associated DC terms ($\Delta_{o,x}$ and q_o respectively), contribute to force noise in the LISA frequency band. To express the force noise contribution of these sources in the frequency domain, the power spectral density (PSD) of charge q and the stray potential difference Δ_x can be calculated. Assuming a Poissonian distribution of the noise, the PSD are defined as follows:

$$S_q = \frac{2e^2\lambda_{\mathrm{eff}}}{4\pi^2 f^2} \tag{19}$$

and for the ASD of charge,

$$S_q^{1/2} = \frac{e\sqrt{2\lambda_{\mathrm{eff}}}}{2\pi f}. \tag{20}$$

Expected values for $S_q^{1/2}$ are $0.6-0.7$ fC$/\sqrt{\mathrm{Hz}}$ at 1 mHz [34]. The term λ_{eff} is defined as the total rate of change in electron charges in the TM, regardless of whether the charge is positive or negative. This quantity depends on two components:

$$\lambda_{\mathrm{eff}} = \lambda_R + \lambda_{\mathrm{cc}}. \tag{21}$$

The term λ_R is the shot noise due to the space environment, which was experimentally determined on LPF. Typical values for λ_{R} was simulated to be 200–400 e/s, and in LPF was actually 1060 ± 90 e/s and 1360 ± 130 e/s for TM 1 and 2, respectively. An average value would be 1210 ± 110 e/s [34]. The λ_{cc} term is the charge shot noise induced on the TM from the charge control operation, which is dependent on the amount of UV light shining into the system from the following expression

$$\lambda_{\mathrm{cc}} = \mathrm{TY}\times P_{\mathrm{UV}}. \tag{22}$$

The term TY is defined as the total yield of all surface pairs within the GRS: TM to housing and TM to each electrode. Note that P_{UV} is used here as the magnitude of the UV power averaged over one second, since the numerical model approximates parameters and approximate noise magnitudes every second. After calculating the contribution from each element, according to the CMS system requirements, the total shot noise λ_{eff} is required to be $\leqslant$5000 e/s [35]. With a measured environment rate $\lambda_{\mathrm{eff},R}$ of 1210 ± 110 e/s, the shot noise due to charge control $\lambda_{\mathrm{eff_{cc}}}$ must be $\lesssim$3800 e/s. Unfortunately the power and amplitude spectral densities of Δ_x, S_{Δ_x} and $S_{\Delta_x}^{1/2}$, do not have explicit analytical expressions and are only determined experimentally through LPF data. The modeling challenge exists because each of the 18 electrodes in the GRS has its own potential, as well as the potential difference between the spacecraft ground and the

TM, which would slightly alter the total potential over time due to system noise (i.e. electronic influence, ground fluctuation, etc). This noise contribution is important to model, as it governs the frequency of the $\delta\Delta_x$ contribution multiplied by the DC charge q_o. Based on LPF data, the ASD of Δ_x is a combination of white noise/Gaussian noise and pink noise ($1/f$). Its noise profile can be defined empirically by the following representation [35]:

$$S_{\Delta_x}^{1/2} = \left(4.5\ \mu\mathrm{V}/\sqrt{\mathrm{Hz}}\right)^2 + \left(190\ \mu\mathrm{V}/\sqrt{\mathrm{Hz}}\right)^2 \left(\frac{0.1\ \mathrm{mHz}}{f}\right)^2 + \left(75\ \mu\mathrm{V}/\sqrt{\mathrm{Hz}}\right)^2 \left(\frac{0.1\ \mathrm{mHz}}{f}\right). \tag{23}$$

Recall from section 1.1 that equation (2), $F_x = -\frac{q}{C_T}\left|\frac{\delta C_x}{\delta_x}\right|\Delta_x$, describes the force on the TM along the measurement x direction [30]. In LPF, the total capacitance of the TM to ground C_T is 34.2 pF and the partial derivative of the total capacitance between the TM and the x-electrode relative to the gap distance x is $\mid \delta C_x/\delta x \mid = 291\ \mathrm{pF\ m^{-1}}$ [34]. Also recall from section 1.1 that the 2nd and 3rd terms of equation (5) are the main sources of noise. To describe these in the frequency domain, we can calculate the ASD of the force due to the noisy charge $S_{F(\delta q)}^{1/2}$, which is the 2nd term, and the ASD of the force due to the noisy electric potential $S_{F(\delta\Delta_x)}^{1/2}$ which is the 3rd term. Using equation (2) the force noise contribution from the noisy charge coupled with a DC presence of Δ_x is equal to the following expression:

$$S_{F(\delta q)}^{1/2}\left(\Delta_x, \lambda_\mathrm{eff}, f\right) = \frac{\Delta_x}{C_\mathrm{T}}\left|\frac{\delta C_x}{\delta x}\right| S_q^{1/2}. \tag{24}$$

Another way to write equation (24) in terms of equations (20)–(22) is:

$$S_{F(\delta q)}^{1/2}\left(P_\mathrm{UV}, f\right) = \frac{\Delta_x}{C_\mathrm{T}}\left|\frac{\delta C_x}{\delta x}\right| \frac{\sqrt{2}e}{2\pi f}\sqrt{\lambda_{\mathrm{eff},e} + \mathrm{TY}\times P_\mathrm{UV}}. \tag{25}$$

Similarly, The force noise contribution from the asymmetrical TM potential difference relative to the housing Δ_x, coupled with a charge contribution q, is equal to the following expression:

$$S_{F(\delta\Delta_x)}^{1/2}\left(q, S_{\Delta_x}^{1/2}\right) = \frac{q_\mathrm{tot}}{C_\mathrm{T}}\left|\frac{\delta C_x}{\delta x}\right| S_{\Delta_x}^{1/2}. \tag{26}$$

When equation (17) is substituted into equation (26) above, the following expression holds:

$$S_{F(\delta\Delta_x)}^{1/2}\left(P_\mathrm{UV}, t, S_{\Delta_x}^{1/2}\right) = \frac{S_{\Delta_x}^{1/2}}{C_\mathrm{T}}\left|\frac{\delta C_x}{\delta x}\right| \left[\left(q_o - q'_\mathrm{eq}\right)\mathrm{e}^{-\frac{\alpha}{C_\mathrm{T}}Pt} + q'_\mathrm{eq}\right]. \tag{27}$$

If the net force noise that the TM is subjected to from all force sources is defined as $S_F^{1/2}$, and if the contribution to force noise from the shot noise from charge q and the stray potential differences Δ_x were only considered, force noise on the Tm would be:

$$S_F^{1/2} = \sqrt{S_{F(\delta q)} + S_{F(\delta\Delta x)}}. \tag{28}$$

6. Simulation results

A number of simulations have been run using the numerical charge model to understand how CMS parameters such as UV light power and phase selection, along with their associated noise components, contributes to LISA performance. The first step of the numerical model is generating a simulated TM potential over time, as detailed in section 6.1. The next step is generating an ASD of the TM potential over time to understand the total contribution of force noise due to the CMS. The force noise result of pulsed continuous charge control mode over 14 days is compared to the DC intermittent mode as featured in section 6.2. To further explore the implications of pulsed continuous mode on the resulting force noise, an analysis on TM stability as a function of UV power and UV noise is summarized in section 6.3, illustrating the force noise result at more than one UV power. To understand the effect of UV power on the TM potential stability, the time domain results as featured in section 6.1 were re-done for various UV powers and is featured in section 6.4, illustrating that there is a tradeoff between UV power and TM potential stability. All time-duration results are done for a 14 day duration coinciding with the intermittent period of discharge nominal for the LPF mission. Another time domain experiment was run for a low (200 pW) and high (2 nW) UV power over the course of 500 days, a factor of 36 longer than all previous results, to show that even the lower UV powers still hold a TM potential below the required 70 mV detailed in section 6.5. All results indicate clear advantages of pulsed continuous mode to be implemented on the future LISA mission over the LPF heritage DC intermittent mode.

6.1. TM potential over 14 days

The nominal UV power proposed for continuous pulsed charge control on LISA is defined by 2 nW, with duty cycles $<36^\circ = 10\%$ [35]. An analysis was done to see what the TM charge drift would be using this power and being subject to the charging environment measured on LPF [13, 36, 37].

First, the phase was adjusted and tuned to bring the TM potential close to 0 V. Looking at the relationship in equation (17), the phase required to produce $q_{\rm ac}$ to compensate for the equilibrium point and the environment to obtain a desired $q'_{\rm eq}$ is governed by the particular light injection port's AY curve, the magnitude of UV power, and the pulse duty cycle. For these experiments, the AY curve used was generated from one of the University of Trento's torsion pendulum UV light injection ports. The University of Trento data was selected because the GRS integrated into their torsion pendulum is a replica of that used in LPF. The UV light injection geometries on the University of Florida torsion pendulum are slightly different from the LPF GRS.

The phase can also be altered to access a larger voltage differential across the TM and electrodes to make the photoelectron bias stronger to help compensate for a changing environment. The particular phase was selected by trial and error running the numerical simulation for a 1–2 h duration and narrowing in on a phase that produced a TM potential as close to 0 V as possible. The method of trial and error could be replaced with explicitly calculating a phase with knowledge of the AY curve and the expected environment charging rate, but for the simulations featured in this work, a trial and error method was used. Once the phase was selected through the trial and error method, the experiment was run for a 14 day duration, which is the average length of time in between TM charge measurements on LPF.

The TM potential with a phase of 201.2° and a 5% duty cycle results in $V_{\rm TM} \approx 3$ m V, and over 14 days slowly drifts up to 3.4 m V when subject to radiation measured on LPF [36, 37], as seen in figure 3. It is interesting to see this slight increase of charge over time. The 2 nW

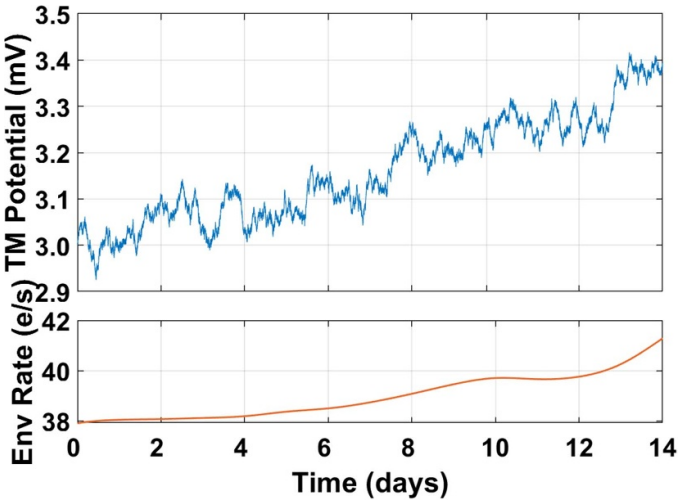

Figure 3. Test mass charge over time using 14 days of LPF charge environment data and 2 nW of UV power with a 5% duty cycle.

of UV power is enough to suppress most environment fluctuations graphed in orange below, but not enough to completely compensate for its gradual increase over this 14 day period. The higher frequency fluctuations in the blue curve are due to approximating the effective noise due to pulsed charge control at every time step of the numerical integration, which is one second.

The simulated TM potential over time is not only interesting for its overall slight drift to positive voltages, but also in the higher frequency variations observed. Ultimately, it is desired to see what the overall force contribution will be due to this continuous discharge nominal mode. Although estimated to perform better in the past, this model is the first of its kind to perform a full nonlinear numerical calculation every second of the TM charge and thus produce the most accurate estimate of sensor performance in the LISA frequency band to date.

6.2. Force Noise Result: Pulsed Continuous Mode vs DC Intermittent Mode

When the amplitude spectral density (ASD) of noise due to δq and $\delta \Delta_x$ is calculated for the pulsed continuous charge control case featured in figure 3, the result is well below the requirement as seen in figure 4. The dark blue curve is the ASD of noise due to the shot noise δq and follows equation (24). Curve fitting was implemented to calculate the resultant shot noise, λ_{eff}, and the error bars were calculated using post-fit residuals.

The total shot noise was 4234 ± 64 e/s, which is below the requirement of 5000 e/s. The sum of the $S^{1/2}_{F(\delta q)}$ blue curve and the $S^{1/2}_{F(\delta \Delta_x)}$ (equation (26)) contribution is the total noise contribution, $S^{1/2}_F$ defined in equation (28). The total noise is dominated by the shot noise, since the $S^{1/2}_{F(\delta \Delta_x)}$ contribution is small because the TM potential is so close to 0 V. If the voltage was larger, the contribution due to shot noise would be larger, as will be seen in the next case. The total noise is a factor of 6 below the requirement for the CMS (orange) and 50 times below the overall LISA noise budget (black). The result proves that pulsed continuous discharge is an advantageous mode of charge control as compared to intermittent charge control, and has the potential of lowering the noise contribution to much below the requirement.

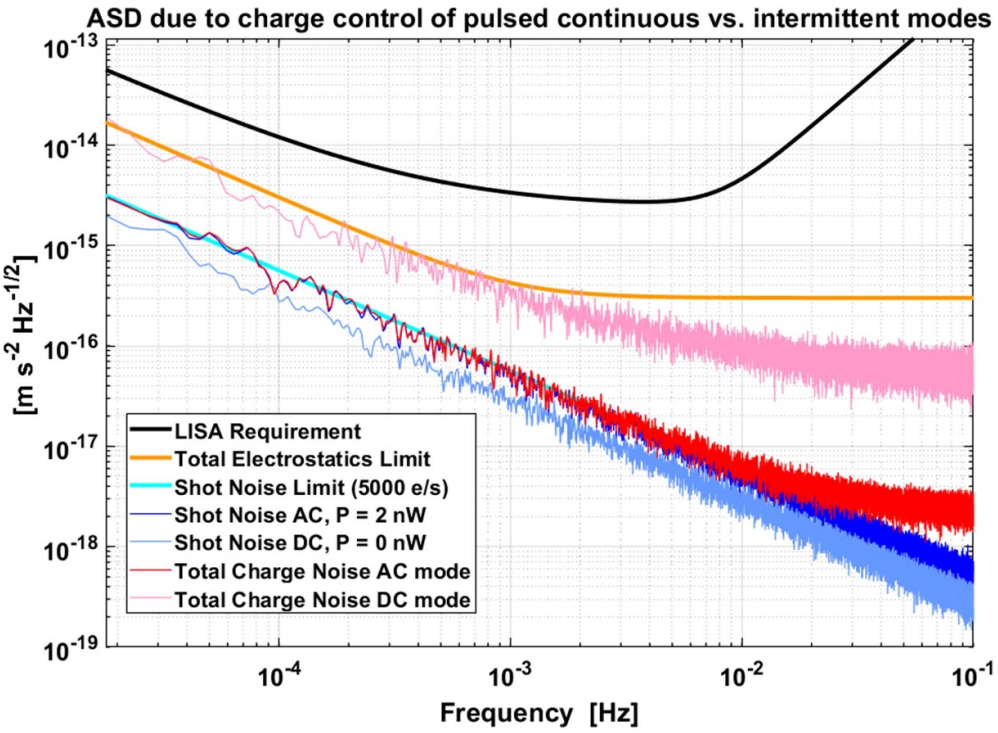

Figure 4. Comparing the amplitude spectral densities of the shot noise (blue) and total charge noise (red) due to continuous charge control to the shot noise (light blue) and total charge noise (pink) due to intermittent charge control exhibited on LPF. Note for continuous mode, the UV light is at 2 nW with a 5% duty cycle and a phase of 201.2° that produces a $V_{\rm TM}$ close to 0 V. For intermittent mode, the UV light is off and the TM potential wanders from −70 m V to 70 m V over the course of 2 weeks.

To compare the advanced mode of charge control to the baseline mode used in LPF, a case was run with the charge dynamics model to simulate the noise performance using intermittent fast (or DC) charge control. In LPF, the TM potential drifted from −70 m V to 70 m V over the course of about 1–3 weeks and intermittent DC discharge was implemented [13]. Having a TM potential at ±70 m V is the limit because if the TM potential goes beyond this level, the ASD due to $\delta\Delta_x$ ($S^{1/2}_{F(\delta\Delta_x)}$) will go beyond the CMS requirement allotment. Thus, as seen in figure 4, the total force due to charge control (pink) is at the same level as the requirement (orange) below 10^{-3} Hz.

In this simulated case, the ASD due to δq (light blue) is only coming from the radiation environment charging, since for intermittent mode, the UV power is off the majority of the time as the charge is left to passively increase, and thus is around the averaged $\lambda_{\rm eff}$ value from LPF of 1210 ± 110 e/s. In this case, the total noise $S^{1/2}_F$ (pink) of intermittent discharge mode is dominated by the $S^{1/2}_{F(\delta\Delta_x)}$ contribution because the shot noise is such a small contribution compared to the noise due to the DC TM potential at the limit of ±70 m V coupled with the noisy electrostatics. However, it is important to note that intermittent discharge mode does not always perform at this noise level. The LPF mission primarily demonstrated intermittent discharge, so when the TM potential was above 70 m V, the UV light had to be turned on to bring the TM voltage back down to −70 m V. Due to a large UV light magnitude, a very large

Table 1. Amplitude Spectral Density of Force Noise at Various UV Powers for Continuous Discharge in units of 10^{-18} m/$\sqrt{\text{Hz}}$.

UV Power	Level at 1 mHz	Level at 0.1 mHz
Requirement	300	2500
3 nW	62.7 ± 8.6	796 ± 75
2 nW	47.1 ± 9.5	422 ± 45
1 nW	49.9 ± 9.9	606 ± 76
500 p W	37.4 ± 6.9	371 ± 37
100 p W	33.8 ± 4.1	333 ± 30
15 p W	33.0 ± 4.5	330 ± 47

amount of shot noise flooded the system and thus pushed the overall noise floor above the LPF requirement, forcing science mode to pause for about 700 s [17]. This is not desirable for the LISA mission because the interruption limits scientific observations of GWs at the lower frequencies beyond 1–3 week timescales [17].

Therefore, if continuous pulsed charge control is possible to implement on LISA, not only would the noise performance of the CMS will be improved by about a factor of 10 from LPF performance, illustrated in the improved noise contribution of the red curve compared to the pink, but it would also enable science mode to run continuously and capture data from lower frequencies. If the CMS produced force noise to these levels on LISA, the mission would have more margin to allow for more noise in other contributions to the overall budget.

6.3. Pulsed continuous mode power analysis

Analyses were done to see how much the force noise on the TM depended on UV power, UV power noise, and UV pulse phase noise. To see if the overall force noise remained below the requirement for the pulsed continuous discharge mode, the TM potential was kept between $1 - 5$ m V and UV powers were tested from 15 p W (which is close to the 10 p W minimum power requirement) to 2 nW (the typical power requirement) and up to 3 nW to approach the maximum allowable for continuous pulsed discharge [38]. As seen in table 1, the force response at 1 mHz and 0.1 mHz remained approximately an order of magnitude below the requirement, with standard deviations indicating the low probability of approaching the requirement.

On LPF, the force noise allocation was frequently approached during intermittent DC charge control even when the UV light was not shining and the TM charge was left to steadily increase from -70 m V to 70 m V over the course of 1–3 weeks [13]. During discharge, the noise allocation was exceeded and thus would degrade the science data in the LISA mission. As seen in these results, pulsed continuous charge control can not only keep the CMS noise contribution lower than on LPF, but can also prevent the science data from being degraded.

6.3.1. Power dependence on phase jitter over power jitter. An analysis was done of the shot noise λ_{eff} contribution of the overall noise was also performed. As previously done, UV powers were swept from 15 p W to 3 nW with 2 nW being the nominal power. The shot noise at each power was calculated with (1) both pulse power noise of $0.1/\sqrt{\text{Hz}}$ and phase jitter of 7 mrad/$\sqrt{\text{Hz}}$ applied (which are the maximum allowable noise requirements from the UV LEDs that the CMS is being designed to [38, 39]), (2) only phase jitter applied and power noise equal zero, and (3) only power noise applied and phase jitter equal zero. As seen in

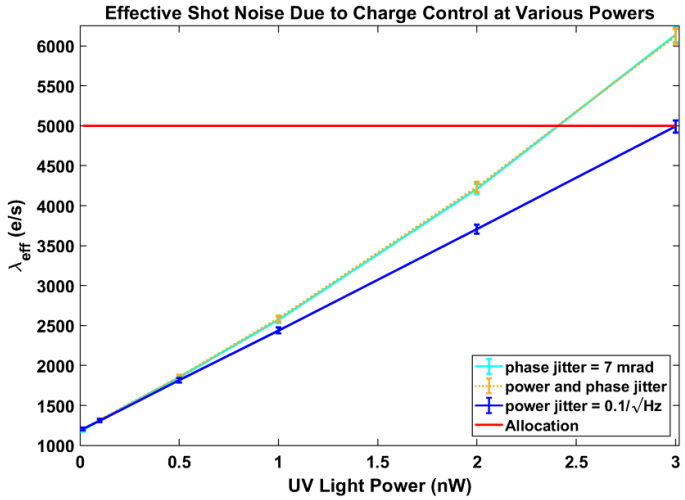

Figure 5. Total shot noise calculated with and without UV power noise and UV pulse phase jitter.

figure 5, the amplitude of λ_{eff} depends more on phase jitter than power noise, as the light blue curve representing only phase jitter applied lines up almost directly with the dotted yellow line corresponding to the case with both noise sources. The maximum allowable relative power noise of $0.1/\sqrt{\text{Hz}}$ and the measured phase jitter noise of 7 mrad$/\sqrt{\text{Hz}}$ are both reasonable assumptions for noise requirements based on the TRL 5 CMS performance [40].

It is seen at powers of 0.5 nW and lower that the shot noise dependence on power noise and phase jitter starts to become sub-dominant compared to the environment shot noise of 1210 ± 110 e/s [34]. This can especially be seen in the standard deviations, which are within the environment average as observed in the whisker bounds featured in the low power data points in figure 5.

6.4. Pulsed Continuous Mode Power Level Optimization

As previously mentioned, based on the CMS requirements, the minimum and maximum UV light powers are 10 p W and 3 nW, respectively [38]. To understand UV light power dependencies beyond what was performed in figure 3, a more detailed analysis was conducted to understand the TM potential drift dependence on UV light power. For this analysis, the same powers were selected as the analysis featured in figure 5. For each power, the UV light phase was selected on a trial and error basis for an hour long observation to keep the TM potential as close to 3–3.5 m V as possible. The simulation was run for a total of 14 days, and can be seen in figure 6.

The lowest powers of 15 p W and 100 p W are shown to diverge more significantly than the UV powers of 500 p W and beyond. Thus, it can be inferred from the analysis that 500 p W would be a good UV power to use since it limits the shot noise while also limiting the TM potential creep on the order of 2 weeks. However, the lowest powers do not creep beyond 8 m V, which is well below the 70 m V requirement and show that even the minimum power requirement of approx. 10 p W will likely outperform the DC intermittent discharge mode.

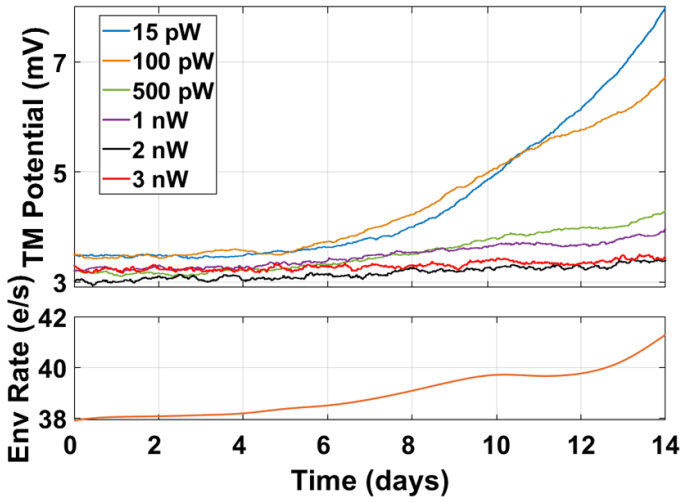

Figure 6. Total shot noise calculated with and without UV power noise and UV pulse phase jitter.

6.5. TM Potential over 500 days

The motivation of the previous results were to compare pulsed continuous charge control mode with DC intermittent discharge model as used on LPF, as well as exploring the effect of UV light noise on overall shot noise and the effect of UV power. In looking ahead to the LISA mission, understanding the effects of pulsed continuous mode over a longer duration than 2 weeks is desired. Thus, the numerical simulation was run for much longer timescales at two UV light powers, 200 p W and 2 nW, to understand the effect of UV light power on the stability of the TM charge long term. The two UV light powers were selected because they represent the two distinct exponential growth curves as seen in figure 6 and are exactly an order of magnitude apart. LPF environment charge rate data was used again [36, 37], but for 500 days, as seen in figure 7.

It can be seen that more TM potential is accrued over 500 days for the 200 p W case. However, the TM potential remains below 23 m V, which is well below the 70 m V requirement. The estimated typical UV light power for LISA is 2 nW, which demonstrates excellent environment charge suppression on the TM over the 500 day span.

7. Future Experimental Work—Torsion Pendulum Validation

The University of Florida Torsion pendulum, modeled after the University of Trento's pendulum, is an instrument to test key charge control effects in a space-like environment [32, 33]. It is composed of a 1 m length, 50 μm tungsten fiber with a cross-bar assembly suspended from it. The entire pendulum assembly is housed in a vacuum chamber kept at a pressure of approximately 6×10^{-4} Pa. The vacuum chamber itself is housed in a thermal room to provide passive temperature stabilization.

The cross-bar is composed of 4 hollow, precision-polished and gold-coated, cubic TMs at the ends with arm lengths of 22 cm. The very low torsional spring constant of the fiber and the the 22 cm arm length of the crossbar makes the pendulum extremely sensitive to forces acting

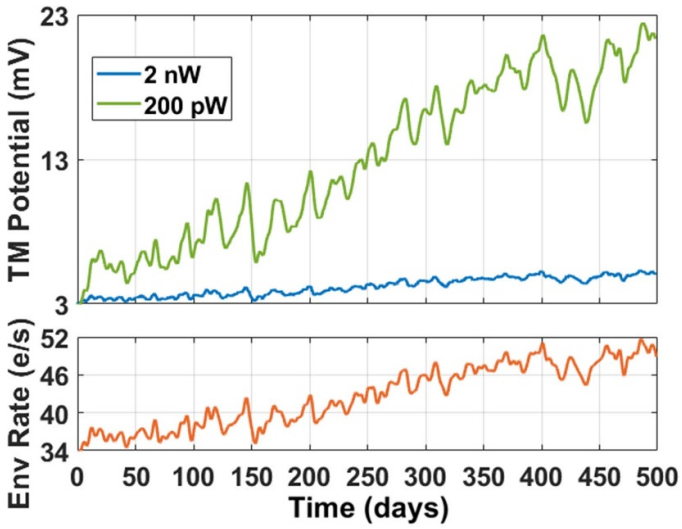

Figure 7. The TM potential drift over a 500 day period with 2 nW of UV power (blue) and 200 pW of UV power (green) when subject to the environment data from LISA Pathfinder (orange).

on the TMs, resulting in a near free-fall condition for the TMs in the translational degree of freedom orthogonal to both the fiber and the crossbar arm.

Two of the four TMs are housed in inertial sensor EHs, with one TM surrounded by a simplified electrode geometry, and the other surrounded by a more representative electrode geometry modeled after LPF. Both GRSs have injection electrodes and sensing electrodes. Both DC and pulsed modes of charge control have been demonstrated in the LISA-like GRS in the UF torsion pendulum [33]. Besides the injection geometries, the LISA-like sensor in the UF torsion pendulum facility is very close in geometry and surface properties to the sensor flown on LPF [41].

There is a laser interferometer readout and a capacitive readout to determine the TM position. The broadband interferometric readout noise is approximately 0.5 $\frac{nm}{\sqrt{\text{Hz}}}$, and the broadband capacitive readout noise is 30 $\frac{nm}{\sqrt{\text{Hz}}}$ [41]. Assuming all forces on the pendulum originate within the inertial sensor, the force on the TM can be calculated using the known geometry and dynamics of the pendulum. See [32] for a detailed description of the pendulum dynamics. The UF torsion pendulum is able to achieve performance down to 2×10^{-13} $\frac{\text{m s}^{-2}}{\sqrt{\text{Hz}}}$ at 1 mHz in the $\hat{x}$ direction using the interferometer readout, a factor of 27 higher than the LISA requirement [33]. Note that this number is the equivalent LISA acceleration noise performance, which is calculated by dividing the measured force acting on the pendulum by the mass of a LISA TM to give the equivalent LISA TM acceleration noise. Therefore, the UF torsion pendulum is an adequate ground-based instrument to test charge control conditions in a space-like environment.

As discussed in the previous section, the charge dynamics model simulates how TM charge changes over time during charge control, and also estimates the frequency dependent electrostatic force noise on the TM. It is desirable to confirm the validity of the model by attempting to match model simulation results to experimental data in the UF torsion pendulum. The model and experimental analysis could be run in parallel to show how having an accurate model of

the GRS system can help predict the desired UV light phase and thus precisely control the TM potential over long periods of time. For example, if it is desired to shift the TM potential to a particular level, the model can simulate the TM potential over time, and through trial and error, the needed phase can be determined.

Unfortunately, due to the fact that the torsion pendulum noise performance is about a factor of 27 above the LISA noise performance requirement and the noise sources coming from the charge control process for low UV light powers and typical applied potential fields are small, experimental results with the UF torsion pendulum were not able to be conducted for the model and simulation work. It is desired to improve the torsion pendulum performance to enable an experimental model verification to inform the selected charge control mode on LISA. Additionally, experimental results could be conducted in the torsion pendulum that amplify the noise due to charge control, such as applying additional electric fields and using large amounts of UV power for discharge and comparing the results to the model. However, this scenario would not be characteristic of a LISA mission flight mode.

8. Future simulation work and operation on LISA

Developing this charge control dynamics simulation model is just the beginning of understanding how pulsed modes will perform in the GRS for LISA. It could also be adapted to accommodate other types of space inertial sensors using pulsed charge control, as long as AY curves for the inertial sensor are known or can be measured. A particular interesting event to simulate with the model would be a solar flare event. It would be helpful to know how the CMS performs with a particular UV power and phase to compensate for such an event. The simulation could help determine the proper UV power level to keep the TM charge constant despite a sudden and large increase in radiation, while also optimizing to keep the shot noise minimal.

Moving ahead with the CMD unit, measured results from the TRL 6 ULU and eventually measured results from flight units can be inserted into the model to predict charge control performance on orbit. The model also operates similarly to how one would operate the CMS on orbit—decide to operate in either continuous or intermittent mode, determine a proper UV light power (and phase if continuous mode selected) to achieve the desired TM charge at a desired time, and then check the charge of the TM to make sure parameters are set properly. The basis of the model presented in this work could help predict how many operational scenarios will perform while LISA is in orbit.

More work can be done to validate the charge dynamics model experimentally, which would be beneficial to the LISA CMS. Measurements of the shot noise are important and could be done using the torsion pendulum. The force response of the pendulum due to charge control operations is possible to measure without improving pendulum performance if the charge noise is amplified such that the resulting force is above the pendulum noise floor. Additionally, measurements of the force on the TM could be measured with artificial increases in the UV pulse power noise and phase jitter, which would validate the numerical simulations of the noise contributions.

9. Conclusion

This paper details an overview of the CMS planned to fly on LISA and the important physics that govern the need for a contact-free method of discharge and the analysis required to ensure instrument performance remains below the requirement. A numerical model was developed

based on analytical expressions to describe how photoelectrons move within the GRS as governed by sensor properties captured in the AY curves, which are generated to perform sensor calibration. An analytical expression and curve fitting tool was also developed to further capture the GRS properties.

It has been shown that pulsed continuous charge control mode is more advantageous than the LPF heritage DC intermittent discharge mode and allows for the spacecraft to have more noise allotment from other subsystems. An interesting analysis was done indicating that reducing the UV phase jitter will have a greater impact on the overall shot noise contribution than reducing the UV power amplitude noise. Additionally, an analysis of different UV light powers were done against LPF environment data, indicating that even the minimum tested UV light power of 15 p W adequately suppresses the environment charge rate over 14 days. A simulated data run was conducted for a long 500 day environmental data exposure and also showed promising results for the pulsed continuous discharge mode, indicating that passive long-term TM charge stability is possible for LISA. In the future, we hope to validate the model using the UF torsion pendulum, as well as explore other possible LISA mission scenarios with the developed numerical charge model.

Data availability statement

The data cannot be made publicly available upon publication because no suitable repository exists for hosting data in this field of study. The data that support the findings of this study are available upon reasonable request from the authors.

Acknowledgment

We would like to acknowledge the funding sources that made this research possible, the NASA LISA Charge Management System Grant 80NSSC17K0277 and NASA N G Roman Technology Fellowship Grant NNX15AF26G.

ORCID iDs

Samantha Parry Kenyon https://orcid.org/0000-0002-5070-6859
Peter J Wass https://orcid.org/0000-0002-2945-399X

References

[1] Touboul P, Foulon B, Christophe B and Marque J P 2012 CHAMP, GRACE, GOCE instruments and beyond *Geodesy for Planet Earth* (Springer) pp 215–21
[2] Ramillien G, Cazenave A and Brunau O 2004 Global time variations of hydrological signals from GRACE satellite gravimetry *Geophys. J. Int.* **158** 813–26
[3] Drinkwater M R, Floberghagen R, Haagmans R, Muzi D and Popescu A 2003 VII: CLOSING SESSION: GOCE: ESA's first earth explorer core mission *Space Sci. Rev.* **108** 419–32
[4] Christophe B, Boulanger D, Foulon B, Huynh P A, Lebat V, Liorzou F and Perrot E 2015 A new generation of ultra-sensitive electrostatic accelerometers for GRACE Follow-on and towards the next generation gravity missions *Acta Astronaut.* **117** 1–7
[5] Everitt C W F *et al* 2015 The Gravity Probe B test of general relativity *Class. Quantum Grav.* **32** 224001
[6] Touboul P *et al* 2017 MICROSCOPE Mission: first results of a space test of the equivalence principle *Phys. Rev. Lett.* **119** 1–7
[7] Danzmann K *et al* 2013 The gravitational universe (arXiv: 1305.5720)

[8] Armano M *et al* 2016 Sub-Femto- g free fall for space-based gravitational wave observatories: LISA pathfinder results *Phys. Rev. Lett.* **116** 1–10
[9] Armano M *et al* 2018 Beyond the required LISA free-fall performance: new LISA pathfinder results down to 20 μHz *Phys. Rev. Lett.* **120** 61101
[10] Amaro-Seoane P *et al* 2017 LISA: laser interferometer space antenna
[11] Abbott B P *et al* 2017 GW170814: a three-detector observation of gravitational waves from a binary black hole coalescence *Phys. Rev. Lett.* **119** 1–16
[12] Shaul D N A, Araujo H M, Rochester G K, Schulte M, Sumner T J, Trenkel C and Wass P 2008 Charge management for LISA and LISA pathfinder *Int. J. Mod. Phys.* D **17** 993–1003
[13] Armano M *et al* 2018 Precision charge control for isolated free-falling test masses: LISA pathfinder results *Phys. Rev.* D **98** 62001
[14] Wass P J, Hollington D, Sumner T J, Yang F and Pfeil M 2019 Effective decrease of photoelectric emission threshold from gold plated surfaces *Rev. Sci. Instrum.* **90** 064501
[15] Olatunde T J 2018 UV LED based charge control for the LISA gravitational reference sensor *PhD Thesis* University of Florida (available at: https://ufdcimages.uflib.ufl.edu/UF/E0/05/40/43/00001/OLATUNDE_T.pdf)
[16] Olatunde T, Apple S, Inchauspé H, Parry S, Letson B, Wass P J and Conklin J W 2020 Characterisation of Au surface properties relevant for UV photoemission- based charge control for space inertial sensors *Class. Quantum Grav.* **37** 195009
[17] Sumner T J, Shaul D N A, Schulte M O, Waschke S, Hollington D and Araújo H 2009 LISA and LISA pathfinder charging *Class. Quantum Grav.* **26** 094006
[18] Letson B C, Barke S, Parry Kenyon S, Olatunde T, Mueller G, Wass P, Ren F, Pearton S J and Conklin J W 2022 High volume UV led performance testing *Rev. Sci. Instrum.* **93** 114503
[19] Xun Sun K, Allard B, Buchman S, Williams S and Byer R L 2006 LED deep UV source for charge management of gravitational reference sensors *Class. Quantum Grav.* **23** S141
[20] Ziegler T, Bergner P, Hechenblaikner G, Brandt N and Fichter W 2014 Modeling and performance of contact-free discharge systems for space inertial sensors *IEEE Trans. Aerosp. Electron. Syst.* **50** 1493–510
[21] Grimani C, Cesarini A, Fabi M and Villani M 2020 Low-energy electromagnetic processes affecting free-falling test-mass charging for lisa and future space interferometers *Class. Quantum Grav.* **38** 045013
[22] Grimani C, Villani M, Fabi M, Cesarini A and Sabbatini F 2022 Bridging the gap between monte carlo simulations and measurements of the lisa pathfinder test-mass charging for lisa *Astron. Astrophys.* **666** A38
[23] Han R *et al* 2024 Study on test-mass charging for taiji gravitational wave observatory *Space Weather* **22** e2023SW003724
[24] Yang F, Hong W, Honggang Li and Ma D 2023 Adaptive charge control for the space inertial sensor *Class. Quantum Grav.* **40** 075004
[25] Wang Y, Tao Y, Wang Z and Liu Y 2023 Photo-electro-thermal model and fuzzy adaptive pid control for UV leds in charge management *Sensors* **23** 5946
[26] Yang F, Hong W, and Zhao Y 2024 Charge management system based on disturbance observer sliding mode control for space inertial sensors (arXiv: 2412.09643)
[27] Inchauspé H, Olatunde T, Apple S, Parry S, Letson B, Turetta N, Mueller G, Wass P J and Conklin J W 2020 Numerical modeling and experimental demonstration of pulsed charge control for the space inertial sensor used in LISA *Phys. Rev.* D **102** 1–15
[28] Hollington D 2011 The charge management system for LISA and LISA pathfinder *PhD Thesis* Imperial College London (available at: www.imperial.ac.uk/media/imperial-college/research-centres-and-groups/high-energy-physics/theses/Hollington.pdf)
[29] Antonucci F, Cavalleri A, Dolesi R, Hueller M, Nicolodi D, Tu H B, Vitale S and Weber W J 2012 Interaction between stray electrostatic fields and a charged free-falling test mass *Phys. Rev. Lett.* **108** 3–7
[30] Weber W J, Carbone L, Cavalleri A, Dolesi R, Hoyle C D, Hueller M and Vitale S 2007 Possibilities for measurement and compensation of stray DC electric fields acting on drag-free test masses *Adv. Space Res.* **39** 213–8
[31] Apple S *et al* 2021 Measurement of stray electric fields via test mass charge modulation
[32] Ciani G, Chilton A, Apple S, Olatunde T, Aitken M, Mueller G and Conklin J W 2017 A new torsion pendulum for gravitational reference sensor technology development *Rev. Sci. Instrum.* **88** 64502

[33] Apple S *et al* 2023 Design and performance characterization of a new lisa-like (laser interferometer space antenna-like) gravitational reference sensor and torsion pendulum testbed *Rev. Sci. Instrum.* **94** 054502
[34] Armano M *et al* 2017 Charge-induced force noise on free-falling test masses: results from LISA pathfinder *Phys. Rev. Lett.* **118** 1–7
[35] Joseph Weber W, Cavalleri A, Bosco D del, Dolesi R, Ferroni V, Riva F, and Russano G 2020 Analysis of LISA electrostatic force and charge management requirements. *Technical Report* (University of Trento)
[36] Wass P J, Sumner T J, Araújo H M and Hollington D 2023 Simulating the charging of isolated free-falling masses from tev to ev energies: detailed comparison with lisa pathfinder results *Phys. Rev.* D **107** 022010
[37] Armano M *et al* 2024 In-depth analysis of lisa pathfinder performance results: time evolution, noise projection, physical models and implications for lisa *Phys. Rev.* D **110** 042004
[38] Doiron T, Thorpe I and Rioux N 2020 LISA Charge Management Device (CMD) Specification *Technical Report* (NASA Goddard Space Flight Center)
[39] Parry Kenyon S *et al* 2021 A charge management system for gravitational reference sensors - design and instrument testing *IEEE Trans. on Aerospace and Electronic Systems, AeroConf*
[40] Parry Kenyon S 2021 Design and simulation of pulsed UV LED charge control for space inertial sensors *PhD Thesis* University of Florida (available at: https://original-ufdc.uflib.ufl.edu/UFE0057812/00001)
[41] Apple S 2020 Design and performance characterization of a new LISA-like gravitational reference sensor testbed using the UF torsion *PhD Thesis* University of Florida (available at: https://original-ufdc.uflib.ufl.edu/UFE0056425/00001)